

EPJ AP

Applied Physics

EPJ.org
your physics journal

Eur. Phys. J. Appl. Phys. **95**, 20501 (2021)

DOI: [10.1051/epjap/2021210121](https://doi.org/10.1051/epjap/2021210121)

Controllable tunneling of planar structures containing single-negative layers

Sergey A. Afanas'ev, Irina V. Fedorova, and Dmitriy I. Sementsov

edp sciences

The title "The European Physical Journal" is a joint property of EDP Sciences, Società Italiana di Fisica (SIF) and Springer

Controllable tunneling of planar structures containing single-negative layers

Sergey A. Afanas'ev^{*}, Irina V. Fedorova, and Dmitriy I. Sementsov

Ulyanovsk State University, ul. L'va Tolstogo 42, 432017 Ulyanovsk, Russia

Received: 4 June 2021 / Received in final form: 20 July 2021 / Accepted: 21 July 2021

Abstract. The possibility of perfect (i.e. non-reflective) tunneling of microwave radiation through planar structures containing layers with negative material parameters is investigated. A symmetric trilayer is considered, including two ferrite layers, which are magnetized by an external field. The conditions of perfect tunneling are obtained analytically using the transfer matrix method. By the numerical solution of the obtained equations, the positions of the highest transmission peaks in the spectrum of the structure are determined. The controllability of the transmission spectra due to the external magnetic field is shown.

1 Introduction

Metamaterials are artificial structures with properties that are beyond the properties of their constituent components. In particular, the material electrodynamic parameters of metamaterials – permittivity ε and permeability μ – can take not only positive, but also negative values. In this regard, such media are referred as single-negative (SNG) or double-negative (DNG) materials [1–3]. If $\text{Re } \varepsilon < 0$ and $\text{Re } \mu > 0$, then the SNG material is called electrically negative (ENG), and in the case of $\text{Re } \varepsilon > 0$ and $\text{Re } \mu < 0$ – magnetically negative (MNG). Materials with both positive ε and μ are denoted as DPS (double-positive).

An electromagnetic wave in SNG material is evanescent (non-propagating) with zero intensity, so such a media are opaque for electromagnetic radiation. This characteristic limits their practical use, because even in the case of minimal losses, they are ineffective [3,4]. However, it is known that the presence of several such layers in the structure (as well as certain their combinations with DPS or DNG layers) makes it possible to obtain almost complete transmission of incident radiation through the structure (“perfect electromagnetic tunneling”) [4–8]. In general, such perfect (non-reflective) tunneling may be reached for any type of waves in various structures supporting evanescent waves when certain matching conditions are met [4,7–11]. Up to date, a lot of various layered tunneling systems containing SNG [4,9,12–15] or DNG [4–6,16–18] layers have been demonstrated to realize the perfect tunneling. Thus, in [9,19–23] for the structures DPS-ENG-DPS it was found that the transmittance reaches values very close to unity in a wide range of values of the angle of incidence of TE and TM polarization radiation. The authors of [23] have demonstrated that by changing the negative permittivity of the middle layer, it is possible to achieve

the existence of fairly wide regions of weak reflection, which, in turn, makes it possible to increase the fraction of absorption by solar cells.

Despite the available results, the problem of selecting the parameters of structures that provide the regime of “near-perfect” tunneling remains relevant. Of particular interest is the possibility of controlling the position of the frequency interval of extremely high transmittance. The tuning ability of refractive index in natural and artificial materials is crucial for numerous photonic applications in different frequency ranges from microwave to visible. Recently, a variety of schemes have been proposed in which the electromagnetic response of a material is controlled by changing the temperature [24,25], external fields [25–29] or illumination [30–32]. Usually, the manipulation of electromagnetic properties is achieved through the introduction of some active media into the material.

In this regard, we study the tunneling of electromagnetic wave through a structure with two magnetically negative (MNG) layers separated by a layer of a nonmagnetic metamaterial with the frequency dispersion of the permittivity. The tunneling of the microwave radiation through similar structures can be near-perfect if the low loss ferrite is used as a MNG medium [27,33–34]. We obtain the conditions of perfect tunneling for the case of negligible losses in the layers of the structure. The obtained solutions of the equations are analyzed depending on the parameters of the structure. Further we find the frequencies at which the transmittance $T \approx 1$ for real lossy trilayer. The changeover of the transmission spectra by external magnetic field is considered.

2 Geometry of the problem and parameters of the structure

Consider a symmetric three-layer structure with layer thicknesses $L_1 = L_3 \neq L_2$. We assume that it is placed in a

^{*} e-mail: asa_rpe@mail.ru

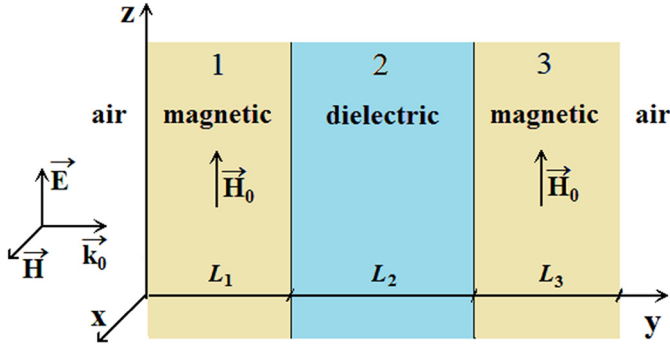


Fig. 1. Geometry of the problem.

vacuum and consists of a central layer 2 of a nonmagnetic (permeability $\mu_2=1$) metamaterial with a frequency dispersion of its permittivity and two adjacent layers 1 and 3 of transversely magnetized ferrite (yttrium iron garnet $\text{Y}_3\text{Fe}_5\text{O}_{12}$). A plane electromagnetic TEM wave is normally incident on the structure from the vacuum. We assume that the normal to the interfaces between the layers and the wave vector k_0 of the incident wave are directed along the Oy axis, and the orientation of the external magnetic field coincides with the direction of the Oz axis (see Fig. 1).

For the frequency dependence of the permittivity of the layer 2, we use the Drude expression [9,20]:

$$\varepsilon(\omega) = 1 - \frac{\omega_p^2}{\omega(\omega - i\Gamma)}, \quad (1)$$

where ω_p is the plasma circular frequency, and Γ is the damping frequency. The sign of the real part ε' of the permittivity (1) depends on the choice of the operating frequency in relation to the plasma frequency. When $\omega < \omega_p$ the layer 2 is an ENG medium, and when $\omega > \omega_p$ it is a DPS medium. In further calculations, the following values of the parameters in (1) were used: $f_p = \omega_p/2\pi = 3.2$ GHz, $\Gamma = 10^{-3}\omega_p$.

In the presence of an external magnetic field in the considered geometry, the permeability of ferrite is anisotropic and is described by a tensor with the components determined by the following expressions [35]:

$$\begin{aligned} \mu_{xx} = \mu_{yy} = \mu &= \frac{\omega_H(\omega_M + \omega_H) - \omega^2}{\omega_H^2 - \omega^2}, \\ \mu_{xy} = -\mu_{yx} = \mu_a &= \frac{i\omega\omega_M}{\omega_H^2 - \omega^2}, \mu_{zz} = 1, \end{aligned} \quad (2)$$

where are entered the parameters $\omega_M = 4\pi\gamma M_s$, and $\omega_H = \gamma H_0$; M_s is the saturation magnetization and $\gamma = 1.76 \cdot 10^7$ Oe $^{-1} \cdot$ s $^{-1}$ is the gyromagnetic ratio. Taking into account losses in (2), the parameter ω_H should be replaced by $\omega_H + i\gamma\Delta H$ (ΔH is the width of the ferromagnetic resonance line). In the numerical simulations, the following ferrite parameters were used: $4\pi M_s = 1850$ G,

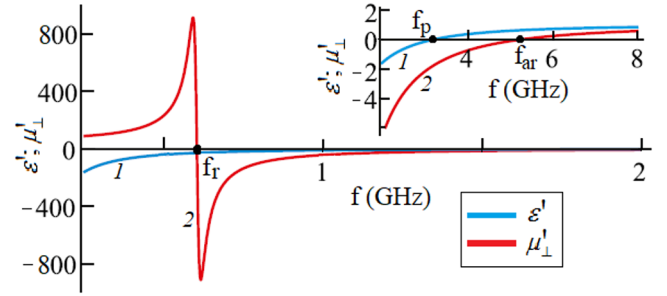


Fig. 2. The material parameters of the structure under study: the real parts of permittivity ε' (1) and effective permeability μ'_{\perp} (2) as functions of frequency at $H_0 = 25$ Oe.

$\Delta H = 1$ Oe, the ferrite permittivity $\varepsilon_f = \varepsilon'_f - i\varepsilon''_f$, where $\varepsilon'_f = 14.8$ and dielectric loss tangent is $\tan \delta = \varepsilon''_f/\varepsilon'_f = 2 \cdot 10^{-4}$.

When a wave propagates perpendicular to the magnetic field H_0 , two eigenwaves with orthogonal polarization, TM and TE, can exist in each of the layers. The characteristics of the TM wave are insensitive to the magnetic field in the ferrite layers; therefore, it is not considered in this work. The features of the high-frequency behavior of the TE wave are largely related to the frequency and field dependence of the effective ferrite permeability

$$\mu_{\perp}(\omega, H_0) = \mu - \mu_a^2/\mu. \quad (3)$$

Its real part μ'_{\perp} is resonantly dependent on frequency; the sign change of μ'_{\perp} occurs at resonance ω_r and antiresonance ω_{ar} frequencies, respectively. Expressions for these specified frequencies are defined as zeros of the function $\mu'_{\perp}(\omega)$:

$$\omega_r = \sqrt{\omega_H(\omega_M + \omega_H)}, \omega_{ar} = \omega_M + \omega_H. \quad (4)$$

In the region $\omega_r < \omega < \omega_{ar}$, the ferrite layers 1 and 3 behave as MNG media, and in the regions $\omega < \omega_r$ and $\omega > \omega_{ar}$ they are DPS ones.

The dependences of the real part μ'_{\perp} of the effective ferrite permeability, as well as of the real part ε' of the central layer permittivity on the frequency $f = \omega/2\pi$ are shown in Figure 2. For the field $H_0 = 25$ Oe chosen for the calculations in Figure 2, the range of negative values of μ'_{\perp} is limited by the frequencies $f_r \approx 0.6$ GHz and $f_{ar} \approx 5.25$ GHz.

Depending on the magnitude of the magnetizing field H_0 , the values of the frequencies f_r and f_{ar} are shifted relative to the fixed value of the plasma frequency f_p . In this regard, three types of the structure under study are possible, which are presented in Table 1.

In this paper, we present an analysis corresponding to the case $f_r < f_p < f_{ar}$ from Table 1, drawn for the frequency regions $f_r < f < f_p$ and $f_p < f < f_{ar}$, where the ferrite is MNG material having $\mu'_{\perp} \leq 0$. The regularities described below, in their basic features, are also preserved for the structures of the other two types.

Table 1. Possible variants of the structure under study.

		1) $f_p < f_r$		
$f < f_p$	$f_p < f < f_r$		$f_r < f < f_{ar}$	$f > f_{ar}$
DPS-ENG-DPS	DPS-DPS-DPS		MNG-DPS-MNG	DPS-DPS-DPS
		2) $f_r < f_p < f_{ar}$		
$f < f_r$	$f_r < f < f_p$		$f_p < f < f_{ar}$	$f > f_{ar}$
DPS-ENG-DPS	MNG-ENG-MNG		MNG-DPS-MNG	DPS-DPS-DPS
		3) $f_p > f_{ar}$		
$f < f_r$	$f_r < f < f_{ar}$		$f_{ar} < f < f_p$	$f > f_p$
DPS-ENG-DPS	MNG-ENG-MNG		DPS-ENG-DPS	DPS-DPS-DPS

3 Conditions of perfect tunneling

Solving the equations of classical electrodynamics for a given geometry of the problem, and then using the boundary conditions, it is possible to obtain a transfer matrix. The matrix of the considered symmetric trilayer has the form $G = N_1 N_2 N_1$. The transfer matrices of individual layers are written as [36]:

$$N_j = \begin{pmatrix} \cos k_j L_j & i \frac{k_j}{k_0 \mu_j} \sin k_j L_j \\ i \frac{k_0 \mu_j}{k_j} \sin k_j L_j & \cos k_j L_j \end{pmatrix}, j = 1, 2, \quad (5)$$

where the wave propagation constants k_j of the waves in the layers denoted by the subscripts j are defined as

$$k_j = k'_j - ik''_j = \pm k_0 \sqrt{\varepsilon_j \mu_j}. \quad (6)$$

Here ε_j and μ_j are permittivities and permeabilities of the layers (which are generally complex), $k_0 = \omega/c$, ω and c are the angular frequency and the speed of the light in vacuum. The square root sign in (6) is chosen so that the imaginary part k''_j is positive, which corresponds to passive (lossy) media.

The fact is that dielectric losses in ferrite are small, and its magnetic losses are significant only in the vicinity of the resonance frequency. By that reason, the conditions of perfect tunneling for lossless structures only are studied in this work. (In such a case the material parameters ε_j and μ_j are real). The conditions of zero reflectance ($R=0$), when the transmittance $T=1$, are obtained when the asymmetric elements of the structure transfer matrix G are equal to zero (i.e. $G_{12} = G_{21} = 0$). The general form of

the components is given by the expression [9]:

See equation (7) below.

where we denote $\zeta_j = k_j/k_0 \mu_j$, $\Phi_j = k_j L_j$.

Taking into account that the wavenumbers are imaginary for SNG media (i.e. $k_j = -ik_0 \sqrt{|\varepsilon_j \mu_j|}$) and they are real for DPS media ($k_j = k_0 \sqrt{\varepsilon_j \mu_j}$), the expressions (6) for the trilayers under investigation can be written as follows:

$$\begin{pmatrix} G_{12} \\ G_{21} \end{pmatrix} = \frac{i}{2Z_2} \begin{pmatrix} -1 \\ 1/Z_1^2 \end{pmatrix} \times \begin{bmatrix} 2Z_1 Z_2 \cosh \varphi_2 \sinh 2\varphi_1 + \begin{pmatrix} 1 \\ -1 \end{pmatrix} (Z_1^2 - Z_2^2) \sinh \varphi_2 \\ -(Z_1^2 + Z_2^2) \cosh 2\varphi_1 \sinh \varphi_2 \end{bmatrix} \quad (8)$$

in the case of MNG-ENG-MNG trilayer and

$$\begin{pmatrix} G_{12} \\ G_{21} \end{pmatrix} = \frac{i}{2Z_2} \begin{pmatrix} -1 \\ 1/Z_1^2 \end{pmatrix} \times \begin{bmatrix} 2Z_1 Z_2 \cos \varphi_2 \sinh 2\varphi_1 - \begin{pmatrix} 1 \\ -1 \end{pmatrix} (Z_1^2 + Z_2^2) \sin \varphi_2 \\ +(Z_1^2 - Z_2^2) \cosh 2\varphi_1 \sin \varphi_2 \end{bmatrix} \quad (9)$$

for MNG-DPS-MNG trilayer. Here $Z_j = \sqrt{|\mu_j/\varepsilon_j|}$ are the absolute values of impedances, $\varphi_j = k_0 n_j L_j$ are the

$$\begin{pmatrix} G_{12} \\ G_{21} \end{pmatrix} = i \begin{bmatrix} \begin{pmatrix} 1/\zeta_1 \\ \zeta_1 \end{pmatrix} \cos \Phi_2 \cos \Phi_3 \sin \Phi_1 + \begin{pmatrix} 1/\zeta_2 \\ \zeta_2 \end{pmatrix} \cos \Phi_1 \cos \Phi_3 \sin \Phi_2 \\ + \begin{pmatrix} 1/\zeta_3 \\ \zeta_3 \end{pmatrix} \cos \Phi_1 \cos \Phi_2 \sin \Phi_3 - \begin{pmatrix} \zeta_2/(\zeta_1 \zeta_3) \\ \zeta_1 \zeta_3 / \zeta_2 \end{pmatrix} \sin \Phi_1 \sin \Phi_2 \sin \Phi_3 \end{bmatrix}, \quad (7)$$

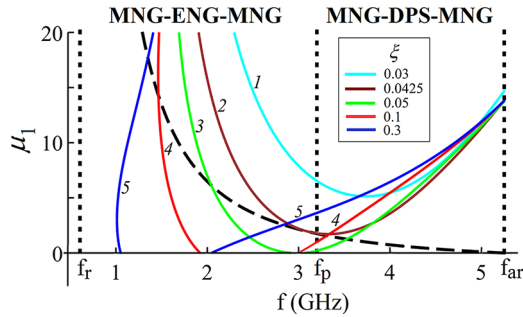


Fig. 3. The solutions of equations (10, 11) at $L_2 = 15$ mm and $\xi = 0.03, 0.0425, 0.05, 0.1, 0.3$ (curves 1–5). The dashed line is the dependence $|\mu_1(f)|$ at $H_0 = 25$ Oe.

effective thicknesses of the layers, $n_j = (|\epsilon_j \mu_j|)^{1/2}$ are the absolute values of complex refractive indices. Thus, the perfect tunneling conditions for MNG-ENG-MNG and MNG-DPS-MNG trilayers take the form of the following equations:

$$\tanh \varphi_2 = \frac{2Z_1 Z_2 \sinh 2\varphi_1}{\left(\frac{1 - Z_1^2}{1 + Z_1^2}\right) (Z_1^2 - Z_2^2) + (Z_1^2 + Z_2^2) \cosh 2\varphi_1}, \quad (10)$$

$$\tan \varphi_2 = \frac{2Z_1 Z_2 \sinh 2\varphi_1}{\left(\frac{Z_1^2 - 1}{Z_1^2 + 1}\right) (Z_1^2 + Z_2^2) - (Z_1^2 - Z_2^2) \cosh 2\varphi_1}. \quad (11)$$

Equations (10) and (11) were solved numerically with respect to the variable μ_1 – the permeability of ferrite layers 1 and 3. Figure 3 shows the frequency dependences of the solutions μ_1 of these equations, obtained for a fixed thickness L_2 of the central layer at various values of dimensionless parameter $\xi = L_1/L_2$. It can be seen that for the structure having fixed values of its geometric parameters, the curves of the solutions of equations (10) and (11) are continuous at frequency f_p separating two corresponding frequency regions. At not too large values of the parameter ξ , one branch is observed (curves 1–3), which has a clearly pronounced minimum. When $\xi > 0.5$, the curves are divided into two branches, and in the interval between them the solutions are absent (curves 4, 5).

On the plot of Figure 3, the dashed line is superposed representing the absolute value of the effective magnetic permeability of ferrite $|\mu_1(f)|$ for a fixed value of the magnetizing field H_0 . The points of intersection of the dashed and solid curves give the frequencies at which near-perfect tunneling will be observed in the transmission spectra of the trilayers. (Deviations from ideality for real structures come out due to the losses). The number of intersections is determined by the choice of the field H_0 and parameter ξ and does not exceed two (with a descending and ascending branch of a curve $\mu_1(f)$). For sufficiently small values of ξ ($\xi < 0.0425$) there are no intersections at all (curve 1).

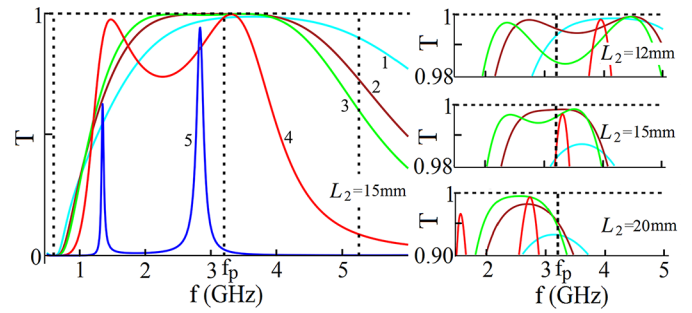


Fig. 4. The transmission spectra of trilayers having different thicknesses L_2 at $H_0 = 25$ Oe, $\xi = 0.03, 0.0425, 0.05, 0.1, 0.3$ (curves 1–5).

4 Transmission spectra of the trilayer

To obtain the transmission spectra of the structure under study, we used the expression for the amplitude coefficient of transmission t , expressed in terms of the elements of the transfer matrix G as

$$t = \frac{2}{G_{11} + G_{12} + G_{21} + G_{22}}. \quad (12)$$

After that, the transmittance $T = |t|^2$ was determined. Calculations in this section were carried out taking into account losses in all layers of the structure, that is, material parameters $\epsilon_{1,2}$ and μ_1 were considered as complex quantities. Since the losses are small enough, the solutions of the conditions (10, 11) obtained for lossless structures give practically exact positions of the transmission peaks in the calculated spectra.

Figure 4 shows the transmittance of the trilayer as function of frequency for three values of the thickness L_2 of the middle layer at different values of the parameter ξ . The calculations were performed for a fixed value of the external magnetic field $H_0 = 25$ Oe. In the following, we analyze in detail the case of $L_2 = 15$ mm, which corresponds to the above Figure 3. At small enough values of ξ , there are no intersections of dashed and solid curves in the plot of Figure 3 and a broad transmission peak is observed in the spectrum (curve 1). In this case, the value of T at the maximum does not reach 1, even if the losses are neglected. If there are two sufficiently close peaks in spectrum, the frequency region represents a “plateau” with an almost constant transmittance close to 1 (curves 2, 3). As the distance between the peaks increases, the left peak shifts noticeably to the resonance frequency and its height decreases due to an increase in magnetic losses. As a result, for relatively large values of ξ (curves 4–5), two well-resolved peaks with a region of low transmission between them are observed.

To increase the bandwidth and the maximum value of transmittance in the “plateau” mode, the thickness L_2 should be reduced. The position of the right peak in a constant magnetic field H_0 strongly depends on it. With increasing L_2 , its gradual transition from the frequency

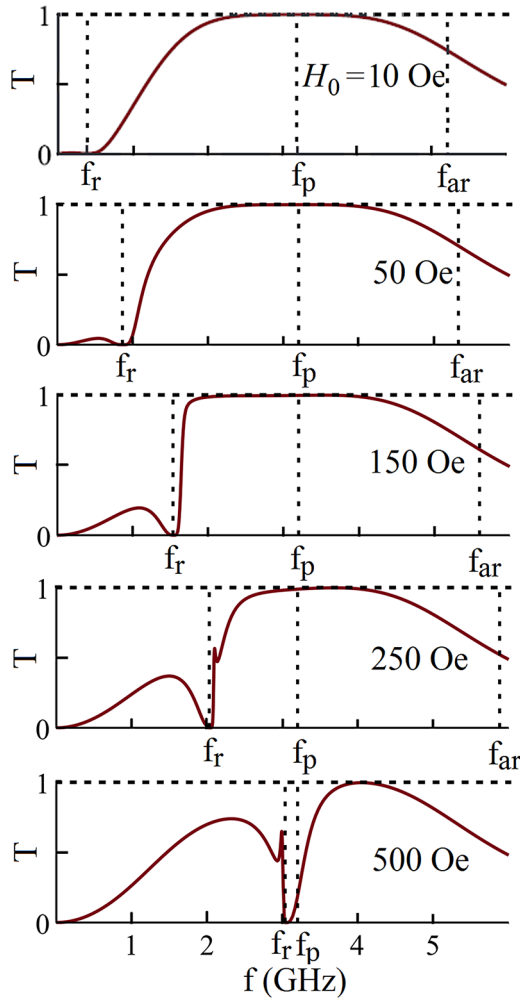


Fig. 5. The transmission spectra of the trilayer having $L_2 = 15$ mm, $\xi = 0.0425$ for different values of magnetizing field.

region $f_p < f < f_{ar}$ to the region of $f_r < f < f_p$ is observed, which leads to a decrease in the bandwidth. It can also be noted that with increasing L_2 , ever larger values of the parameter ξ are required to get a “plateau” in the transmission spectrum.

Since the structure includes ferrite layers, its transmission spectra can be effectively controllable by the magnetizing field. In Figure 5 one can see how the bandwidth is tuned when the value of H_0 changes in the most interesting situation, when there is a “plateau” between two peaks of transmittance. In the range of fields up to approximately $H_0 = 150$ Oe, the bandwidth and the position of the “plateau” change only slightly. In stronger magnetic fields, the frequency region $f_r < f < f_p$ is noticeably reduced, and the left peak participating in the formation of the “plateau” approaches the right one, the position of which is almost independent of H_0 . Thus, the bandwidth becomes narrower. In sufficiently large fields, as the value of f_r tends to f_p , the two peaks merge into one observed in the region $f_p < f < f_{ar}$.

5 Conclusion

The paper presents the results of numerical simulation of the tunneling of a plane TEM wave through a symmetric trilayer formed by two magnetically negative layers and a metamaterial layer between them, which has a frequency dispersion of the permittivity according to Drude’s law. It is shown that this structure allows one to observe near-perfect tunneling if the parameters of its layers are matched to meet certain conditions. Equations expressing these conditions are obtained and the results of their numerical solution are analyzed. It was found that the transmission spectra of the structure have two peaks with a transmittance close to 1 in the region of negative effective permeability of ferrite. In addition to the situation of two isolated peaks, it is possible to obtain a wide bandwidth between them with a high transmission coefficient. It was found that the width of this bandwidth can be effectively controlled by changing the magnetizing field.

This work was supported by the Ministry of Education and Science of the Russian Federation (Mega-grant program, application #2020-220-08-1369; project #0004-2019-0002) and the Russian Foundation for Basic Research (project #18-29-19101).

Author contribution statement

S.A. Afanas’ev and I.V. Fedorova performed the modeling. The results were discussed jointly by all authors. The paper was organized by D.I. Sementsov, S.A. Afanas’ev wrote the manuscript and I.V. Fedorova designed the figures. All the authors commented on previous version and approved the final version of the manuscript.

References

1. N. Engheta, R.W. Ziolkowski, *Metamaterials: Physics and Engineering Explorations* (Wiley and IEEE Press, Hoboken, 2006)
2. C. Caloz, T. Itoh, *Electromagnetic Metamaterials: Transmission Line Theory and Microwave Applications* (Wiley Interscience, Hoboken, 2006)
3. R. Marques, F. Martin, M. Sorolla, *Metamaterials with Negative Parameters: Theory, Design, and Microwave Applications* (Wiley Interscience, N.Y., 2008)
4. A. Alu, N. Engheta, *IEEE Trans. Antennas Propag.* **51**, 2558 (2003)
5. J.D. Baena, L. Jelinek, R. Marques, F. Medina, *Phys. Rev. B* **72**, 075116 (2005)
6. J.D. Baena, L. Jelinek, R. Marques, *New J. Phys.* **7**, 166 (2005)
7. J. Park, K.-Y. Kim, B. Lee, *Phys. Rev. A* **79**, 023820 (2009)
8. L. Jelinek, J.D. Baena, J. Voves, R. Marques, *New J. Phys.* **13**, 083011 (2011)
9. E. Cojocaru, *Prog. Electromagn. Res.* **113**, 227 (2011)
10. J. Zheng, Y. Chen, Z. Chen, *Opt. Express* **21**, 16742 (2013)
11. L. Wei, *Mater. Res. Express* **3**, 126201 (2016)

12. W. Tan, Z.G. Wang, H. Chen, Prog. Electromagn. Res. M **8**, 27 (2009)
13. C.H. Liu, N. Behdad, Prog. Electromagn. Res. M **42**, 1 (2012)
14. T. Feng, Y. Li, H. Jiang, Phys. Rev. E **79**, 026601 (2009)
15. K.W. Eccleston, I.G. Platt, Electronics **8**, 1 (2019)
16. H. Daninthe, S. Foteinopoulou, C.M. Soukoulis, Phot. Nanostr. **4**, 123 (2006)
17. C. Sabah, H.T. Tastan, F. Dincer, K. Delihacioglu, M. Karaaslan, E. Unal, Prog. Electromagn. Res. **138**, 293 (2013)
18. S.A. Afanas'ev, D.I. Sementsov, Y.V. Yakimov, Opt. Commun. **369**, 164 (2016)
19. C. Yang, H. Zhao, Cent. Eur. J. Phys. **11**, 594 (2013)
20. G. Castaldi, I. Gallina, V. Galdi, A. Alu, A. Engheta, Phys. Rev. B. **83**, 081105 (2011)
21. Y. Chen, S. Huang, X. Yan, J. Shi, Chin. Opt. Lett. **12**, 101601 (2014)
22. L. Zhou, W. Wen, C.T. Chan, P. Sheng, Phys. Rev. Lett. **94**, 243905 (2005)
23. N.N. Beletskii, S.A. Borysenko, Telecomm. Radio Eng. **76**, 1613 (2017)
24. F. Ling, Z. Zhong, R. Huang, B. Zhang, Sci. Rep. **8**, 1 (2018)
25. S.A. Afanasiev, D.A. Evseev, D.I. Sementsov, Opt. Spectrosc. **127**, 468 (2019)
26. L. Ju, B. Geng, J. Horng et al., Nat. Nanotechnol. **6**, 630 (2011)
27. A.V. Strashevskiy, V.B. Kazanskiy, V.R. Tuz, Radio Phys. Radio Astron. **16**, 192 (2011)
28. S.H. Lee, J. Choi, H.-D. Kim, H. Choi, B. Min, Sci. Rep. **3**, 2135 (2013)
29. V. Sorathiya, V. Dave, Opt. Comm. **456**, 124581 (2020)
30. S.E. Harris, A.V. Sokolov, Phys. Rev. A. **55**, R4019 (1997)
31. N. Boutabba, H. Eleuch, Results Phys. **19**, 103421 (2020)
32. N. Boutabba, J. Opt. in press (2021)
33. S.A. Afanas'ev, D.I. Sementsov, I.V. Fedorova, Tech. Phys. **62**, 1848 (2017)
34. S.A. Afanas'ev, I.V. Fedorova, D.I. Sementsov, Prog. Electromagn. Res. M **88**, 33 (2020)
35. A.G. Gurevich, G.A. Melkov, *Magnetic Oscillations and Waves* (Fizmatlit, Moscow, 1994)
36. M. Born, E. Wolf, *Principles of Optics: Electromagnetic Theory of Propagation, Interference and Diffraction of Light*, 7th edn. (Cambridge University Press, Cambridge, 1999)

Cite this article as: Sergey A. Afanas'ev, Irina V. Fedorova, Dmitriy I. Sementsov, Controllable tunneling of planar structures containing single-negative layers, Eur. Phys. J. Appl. Phys. **95**, 20501 (2021)